PUBLICATIONS OF THE ASTRONOMICAL SOCIETY OF THE PACIFIC, **111**:1298–1315, 1999 October

Panoramic Polarimetry Data Analysis

WILLIAM B. SPARKS[1] AND DAVID J. AXON[2]
Received 1999 April 15; accepted 1999 June 28

ABSTRACT. Derivation of accurate polarization information about an astronomical target is a vital tool for investigation of astrophysical processes. Use of large area detectors for imaging and spectroscopy has become commonplace, and frequently such instruments offer a polarization capability. Processing of polarimetric data, however, is nontrivial, especially when the polarimeter is far from ideal. Here we present an overview of the analysis procedures needed to properly process polarimetry data that comprise a series of images of an object taken through a given set of polarizers, such as the imaging instruments on the *Hubble Space Telescope* (*HST*). The analysis can also be used for other types of polarization data, such as spectra. We consider only linear polarization, not circular. The polarizers do not need to be perfect polarizers, although it is important that their characteristics be well established. From an input data set of n intensities (or, equivalently, fluxes) and their errors, assumed independent between observations, corresponding to a set of observations through n polarizers (not necessarily identical or perfect), we show how to derive the Stokes parameters and their covariance matrix both for the special case of $n = 3$ and for general n.

We then discuss how to derive higher level parameters such as polarization degree and position angle and their associated uncertainties and indicate ways to "debias" the positive definite polarization degree. We present tests of our analysis using Monte Carlo simulations. Finally, we show the achievable accuracy for various levels of polarization and signal-to-noise ratio for typical cases, which should be useful for observation design. The techniques allow accurate recovery of polarization information from several of the instruments on board the *HST* as well as estimates of the uncertainties in the results.

1. INTRODUCTION

Astronomical observations of polarized light (used loosely for any electromagnetic radiation here) can often provide important insights into physical processes which are relevant to the phenomena we study and maybe even to the origin of life itself (Bailey et al. 1998). Polarization, a preferential direction of oscillation for the electromagnetic vector, can be induced intrinsically through the radiation process itself (Collett 1993). An example of this is the exceptionally high degree of linear polarization (henceforth polarization; we do not consider circular polarization here) found in the synchrotron-emitting Crab Nebula or the jet of M87 (see, e.g., Perlman et al. 1999). Polarization can also be introduced by the propagation of radiation through a medium that itself has a preferred orientation. The most common example of this, perhaps, is the transmission of light through dust grains aligned by Galactic magnetic fields (Mathewson & Ford 1971; Axon & Ellis 1976). The third way in which light can become polarized is through scattering by a medium. For example, in molecular clouds one frequently "sees" radiation that is scattered by dust in the vicinity of an object which is itself invisible due to extreme obscuration along the line of sight to the observer (see, e.g., Gledhill, Chrysostomou, & Hough 1996). Scattered light is seen in the nuclear regions of active galaxies (Antonucci & Miller 1985; Capetti et al. 1995) and from supernovae that erupted and are now gone, but where light travel time delays allow us still to see the light echo of the original event (Sparks 1994; Schmidt et al. 1994; Sparks et al. 1999). In these cases, the polarization is enabling a precious opportunity in astronomy, namely, the ability to view a distant target from another angle (see, e.g., Henney, Raga, & Axon 1994).

Often polarization observations are obtained of single point sources using exceedingly accurate, dedicated polarimeters (see, e.g., Hough, Peacock, & Bailey 1991). For the interesting cases where the polarized light is extended, it is necessary to use "imaging polarimetry" observations. In principle, polarization observations simply require the introduction of polarizing optics before a camera. For example, Sparks et al. (1989, 1990) used four polarizing filters placed in the collimated beam of the

[1] Visiting Scholar, Center for Astrophysical Sciences, The Johns Hopkins University, 3400 North Charles Street, Baltimore, MD 21218; on sabbatical leave from Space Telescope Science Institute; sparks@stsci.edu.
[2] Department of Physical Sciences, University of Hertfordshire, Hatfield, Herts, AL10 9AB, England, UK; dja@star.herts.ac.uk.

EFOSC camera at the European Southern Observatory. On the ground this technique may be hampered by atmospheric variations, as transmission and point-spread function change between the multiple observations required to obtain the Stokes parameters Q and U.

Traditionally this problem has been overcome by using dedicated two-beam polarimeters (see, e.g., Scarrott et al. 1983), in combination with some kind of rotating retarding plate, so that a complete Stokes parameter set can be obtained at any one time. In contrast with the removal of the atmospheric effects by such means, space-based imaging polarization observations have almost exclusively used multiple polarizing filters of various degrees of sophistication, so as to eliminate the potential "single point failure" possible with rotating elements such as wave plates. The exceedingly stable observational environment essentially eliminates the need for simultaneous acquisition of the complete Stokes parameter set.

Examples include the three double Rochon prism polarizers (essentially perfect polarizers from 300 to 600 nm, but with different efficiencies shortward of 300 nm) housed in the Faint Object Camera (FOC) on board the *Hubble Space Telescope* (*HST*). Other *HST* instrumentation utilizing three polarizers oriented at different position angles are the Near Infrared Camera and Multi Object Spectrometer (NICMOS) and the Advanced Camera for Surveys (ACS), due to be launched around the year 2000 (Ford et al. 1998). The Wide Field and Planetary Camera 2 (WFPC2) also has a polarization capability where images can be taken with a variety of position angles at a variety of detector locations using a polarizing "quad" filter. In the case of both WFPC2 and NICMOS, the polarimeters are far from perfect, either because of the poor polarizing characteristics of the polarizing elements or because of misalignment from the ideal choice of position angles (0°, 60°, and 120° are ideal if three observations are used). WFPC2 can be used with "partial rotations" that are far from ideal, and NICMOS suffers from both polarizer inefficiencies and small angle misalignments.

Processing of such data with imperfect polarizers is a classic problem. Here we attempt to offer a "top-to-bottom" analysis for the case of observations using n general polarizers (§ 2), making full allowance for polarizer inefficiencies. We solve the equations for the Stokes parameters in the general case of n potentially imperfect polarizers, including expressions for the covariances of those parameters (§ 3) for the special case of three polarizers and (§ 4) for n. We proceed in § 5 to derive estimates of the polarization degree and position angle, using transformations of the Stokes parameters which lead to data having a standard Rice distribution and which hence allow existing methods of debiasing the positive definite polarization degree to be applied (Simmons & Stewart 1985). We also use similar transformations that enable us to estimate the uncertainties on these parameters (§ 6). We present tests of the analysis, and graphs of achievable accuracy under various circumstances in § 7. These are intended for use in observational design. It transpires, not unexpectedly, that the achievable accuracy is a function of the mean signal-to-noise ratio (S/N) times polarization degree, which we call $\eta \equiv p\langle \mathrm{S/N} \rangle$, where $\langle \mathrm{S/N} \rangle$ is the average S/N per image.

We do not present an exhaustive account of the effects of non-Gaussian statistics on the input data, although we do compare Poisson uncertainties to Gaussian using simulations. Nor do we devote time to "instrumental polarization," which should be taken out after derivation of the Stokes parameters (Tinbergen 1996; Biretta & McMaster 1997). Additionally, we do not take into account mismatches between point-spread functions from polarizer to polarizer, and we assume the polarizers have been well characterized and properly calibrated.

2. INPUT DATA AND ASSUMPTIONS, CHARACTERISTICS OF POLARIZERS

2.1. Linearly Polarized Light

There are numerous sources of reference for a detailed introduction to polarimetry, e.g., Tinbergen (1996). Here we give only a brief outline of the basics, and only for linearly polarized light.

Linearly polarized light requires measurement of three quantities to characterize it fully. These can be expressed in a variety of ways. They are the total intensity of the light I, the degree of polarization p, and the position angle of polarization θ. Frequently used, and essential in this work, are the Stokes parameters (I, Q, U), which may be thought of as an "intermediate" stage between the input data and the solution of polarization quantities. These quantities are related through

$$Q = Ip \cos 2\theta , \qquad U = Ip \sin 2\theta ,$$

or the other way around,

$$p = \frac{(Q^2 + U^2)^{1/2}}{I} , \qquad \theta = \frac{1}{2} \tan^{-1} \left(\frac{U}{Q} \right) .$$

Note that these are all intrinsic properties of the source of radiation and should not be confused with the properties of the polarizing elements.

2.2. Polarizing Element Characteristics

A linearly polarizing element also requires three quantities to characterize its behavior or response fully. These are essentially its efficiency as a polarizer (i.e., the ability to reject and accept polarized light of perpendicular and parallel orientations), its overall throughput, in particular to unpolarized light, and the position angle of the polarizer. There are a variety of conventions commonly used to present these three quantities—for example, they can be expressed as the characteristics of a single polarizing element or as the properties of a pair of elements in series. Mazzuca et al. (1998) offer conversions between three such conventions.

Here, we adopt the convention that the output intensity of a beam with input Stokes parameters (I, Q, U) passing through a polarizing element is given by

$$I_k = \frac{1}{2} t_k[I + \epsilon_k(\cos 2\phi_k Q + \sin 2\phi_k U)] , \tag{1}$$

where the subscript k anticipates that the polarizing element is the kth of a series, t is related to the throughput to unpolarized light, ϵ is the efficiency of the polarizer, and ϕ is the position angle of the polarizer. Mazzuca et al. (1998) give the conversions between this characterization of polarizing elements and two others. For example, with three perfect polarizers at optimal orientation, we could have $t_k = 1$, $\epsilon_k = 1$, $(\phi_1, \phi_2, \phi_3) = (0°, 60°, 120°)$. This would be a good approximation to the FOC polarizers mentioned above. Another example is a perfectly *bad* polarizer, e.g., a piece of high-quality glass, where we would have $t_k = 2$, $\epsilon_k = 0$, and the ϕ_k values can be anything (since ϵ is zero). This example is not absurd: in the case of n polarizers of arbitrary characteristics, discussed below in § 4, it may be used to include as part of the observing sequence a direct observation of the target without any polarizing element in beam. Then the formula below will allow this additional observation to form part of the derivation of polarization quantities to maximize the obtainable S/N.

2.3. Input Data and Assumptions

We assume that we have made a set of n observations of a source, each using a polarizing element of arbitrary but known characteristics. This could include observations without any polarizer or repeat observations with the same polarizer. However, at least three observations must be made using polarizers of *different characteristics* to allow solution for the three unknowns in the description of the polarization of the incoming light. Let the measured intensity through the kth polarizer be I_k, as above.

We assume that each observation is independent of the other observations. This is expected to be the case in most instances. Note that it does not necessarily imply that the derived Stokes parameters will be independent of one another.

We also require that the uncertainty associated with the measurement I_k be known, which we denote as σ_k. Our error analysis will assume σ is normally distributed, for the analytic work, and we include Poisson distributed in the Monte Carlo simulations.

3. THE CASE OF THREE POLARIZERS

3.1. Solution of Linear Equations

The minimum number of polarization observations required to determine the three unknowns represented by the Stokes parameters is obviously three. With a high demand on time and desire for efficient observing, this has driven the normal imaging polarization observing mode for *HST*, at least, to be three polarizers at approximately 60° orientation with respect to one another. The FOC uses double Rochon prisms with exceptionally good polarizing characteristics, oriented close to a 60° spacing from one another (Nota et al. 1996). These prisms can be used in combination with other optical elements to allow polarization to be measured at different wavelengths. The NICMOS has two sets of three polarizers that cannot be used in combination with other optical elements. One set is for the shorter wavelengths and the other for the longer wavelengths. These polarizers do not have the characteristics of perfect polarizers, having lowered efficiency and nonoptimal orientations. However, with appropriate characterization they may still be used to excellent effect (Hines 1998). The ACS is also expected to possess two sets of three polarizers. These comprise polaroid material with one set optimized for use in the blue and the other for use in the red. It will be possible to use these polarizers in conjunction with other optical elements.

WFPC2 requires a more complex set of observations (Biretta & McMaster 1997) and may be considered appropriate to the general case discussed in § 4 below, while *HST* Space Telescope Imaging Spectrograph does not have a polarization capability.

Equation (1) above with k in the range 1–3 gives three equations for the three unknowns, (I, Q, U). To be quite clear, we write

$$I_1 = \frac{1}{2} t_1[I + \epsilon_1(\cos 2\phi_1 Q + \sin 2\phi_1 U)] , \tag{1a}$$

$$I_2 = \frac{1}{2} t_2[I + \epsilon_2(\cos 2\phi_2 Q + \sin 2\phi_2 U)] , \tag{1b}$$

$$I_3 = \frac{1}{2} t_3[I + \epsilon_3(\cos 2\phi_3 Q + \sin 2\phi_3 U)] . \tag{1c}$$

This straightforward linear system may be explicitly solved (see, e.g., Hines 1998) to yield

$$(I, Q, U) = A \begin{pmatrix} I_1 \\ I_2 \\ I_3 \end{pmatrix} , \tag{2}$$

or to introduce a minor simplification

$$(I, Q, U) = B \begin{pmatrix} I_1^* \\ I_2^* \\ I_3^* \end{pmatrix} , \tag{3}$$

where $I_k^* = I_k/(0.5t_k)$ (i.e., the matrix A is the matrix B with rows divided by $0.5t_k$) and the matrix B is given by

$$B = \begin{pmatrix} \epsilon_2 \epsilon_3 \sin (2\phi_3 - 2\phi_2) & \epsilon_1 \epsilon_3 \sin (2\phi_1 - 2\phi_3) & \epsilon_1 \epsilon_2 \sin (2\phi_2 - 2\phi_1) \\ \epsilon_2 \sin 2\phi_2 - \epsilon_3 \sin 2\phi_3 & \epsilon_3 \sin 2\phi_3 - \epsilon_1 \sin 2\phi_1 & \epsilon_1 \sin 2\phi_1 - \epsilon_2 \sin 2\phi_2 \\ \epsilon_3 \cos 2\phi_3 - \epsilon_2 \cos 2\phi_2 & \epsilon_1 \cos 2\phi_1 - \epsilon_3 \cos 2\phi_3 & \epsilon_2 \cos 2\phi_2 - \epsilon_1 \cos 2\phi_1 \end{pmatrix} / \Omega , \tag{4}$$

where

$$\Omega = \epsilon_1 \epsilon_2 \sin (2\phi_2 - 2\phi_1) + \epsilon_2 \epsilon_3 \sin (2\phi_3 - 2\phi_2) + \epsilon_1 \epsilon_3 \sin (2\phi_1 - 2\phi_3) .$$

3.2. Associated Covariance Matrix

If each of the I_k measurements has an associated variance of σ_k^2, then the covariance matrix for the (I, Q, U) vector is given by

$$\sigma_{ij}^2 = \sum_k A_{ik} A_{jk} \sigma_k^2 . \tag{5}$$

This is a sum of coefficients times variances of the input observables. For example, the variance on Q is obtained by setting $i = j = 2$ and summing over k. More explicitly,

$$\sigma_I^2 = A_{11}^2 \sigma_1^2 + A_{12}^2 \sigma_2^2 + A_{13}^2 \sigma_3^2 , \qquad \sigma_Q^2 = A_{21}^2 \sigma_1^2 + A_{22}^2 \sigma_2^2 + A_{23}^2 \sigma_3^2 , \qquad \sigma_U^2 = A_{31}^2 \sigma_1^2 + A_{32}^2 \sigma_2^2 + A_{33}^2 \sigma_3^2 .$$

The covariance terms of the matrix give information on the expected dependencies of the derived Stokes parameters on one another. Another way to express this covariance is through the more familiar (linear, Pearson) correlation coefficient (which lies between 0 and 1 in absolute value for zero to perfect correlation), $R_{ij} = \sigma_{ij}^2/\sigma_i \sigma_j$, where σ_{ij}^2 is the covariance between vector elements i and j. As above, we have the covariances

$$\sigma_{IQ}^2 = A_{11} A_{21} \sigma_1^2 + A_{12} A_{22} \sigma_2^2 + A_{13} A_{23} \sigma_3^2 ,$$

$$\sigma_{IU}^2 = A_{11} A_{31} \sigma_1^2 + A_{12} A_{32} \sigma_2^2 + A_{13} A_{33} \sigma_3^2 ,$$

$$\sigma_{QU}^2 = A_{21} A_{31} \sigma_1^2 + A_{22} A_{32} \sigma_2^2 + A_{23} A_{33} \sigma_3^2 .$$

The variances are obviously essential in a proper error analysis, and the covariances will also be used in order to derive estimates of the higher level quantities such as polarization degree from the Stokes parameters. For perfect polarizers oriented at 60° to one another, the covariances are close to zero. If the polarizers are perfect and the uncertainties on each observation are all equal, then the covariances are zero, otherwise a small covariance is introduced because of the different weighting of each observation.

4. THE CASE OF *n* POLARIZERS

We now turn to the case of n polarizers and derive an analogous solution. Note the obvious: we still seek only three unknowns, and hence the associated covariance matrix is still a 3×3 matrix as above. We will adopt a maximum likelihood approach, which is equivalent to a least-squares minimization.

Suppose the true underlying values of the Stokes parameters of the source are (I, Q, U). Then we would expect to observe a mean intensity through the kth polarizer of I'_k as in equation (1):

$$I'_k = \frac{1}{2} t_k[I + \epsilon_k(\cos 2\phi_k Q + \sin 2\phi_k U)] . \qquad (6)$$

Hence the likelihood of observing a particular value I_k, given an underlying mean of I'_k, is

$$\rho_k = \frac{1}{\sqrt{2\pi}\sigma_k} e^{-(I_k - I_k')^2/2\sigma_k^2} ,$$

and hence the likelihood of observing a set of n values $\{I_k\}$ is

$$\rho = \rho_1 \rho_2 \dots \rho_n , \qquad \rho = \rho_0 \exp\left[-\frac{(I_1 - I'_1)^2}{2\sigma_1^2} - \frac{(I_2 - I'_2)^2}{2\sigma_2^2} - \frac{(I_3 - I'_3)^2}{2\sigma_3^2} - \dots \right],$$

where ρ_0 is a constant. Maximizing the likelihood function ρ is equivalent to minimizing the absolute value of the exponent, which is a sum of normalized deviations from the mean value. That is, the "least-squares" estimate. Hence the problem becomes minimize

$$\chi^2 = \frac{1}{2} \sum_k \frac{(I_k - I'_k)^2}{\sigma_k^2} . \qquad (7)$$

The values of I'_k can be substituted into equation (7) from equation (6), and minimization of χ^2 is obtained by taking partial derivatives with respect to each of I, Q, U in turn and equating to zero. Algebraic manipulation leads to a set of three equations

$$\sum \frac{I_k t_k}{\sigma_k^2} = \frac{1}{2} \sum \frac{t_k^2}{\sigma_k^2} I + \frac{1}{2} \sum \frac{t_k^2 \epsilon_k \cos 2\phi_k}{\sigma_k^2} Q + \frac{1}{2} \sum \frac{t_k^2 \epsilon_k \sin 2\phi_k}{\sigma_k^2} U ,$$

$$\sum \frac{I_k t_k \epsilon_k \cos 2\phi_k}{\sigma_k^2} = \frac{1}{2} \sum \frac{t_k^2 \epsilon_k \cos 2\phi_k}{\sigma_k^2} I + \frac{1}{2} \sum \frac{t_k^2 \epsilon_k^2 \cos^2 2\phi_k}{\sigma_k^2} Q + \frac{1}{2} \sum \frac{t_k^2 \epsilon_k^2 \sin 2\phi_k \cos 2\phi_k}{\sigma_k^2} U ,$$

$$\sum \frac{I_k t_k \epsilon_k \sin 2\phi_k}{\sigma_k^2} = \frac{1}{2} \sum \frac{t_k^2 \epsilon_k \sin 2\phi_k}{\sigma_k^2} I + \frac{1}{2} \sum \frac{t_k^2 \epsilon_k^2 \sin 2\phi_k \cos 2\phi_k}{\sigma_k^2} Q + \frac{1}{2} \sum \frac{t_k^2 \epsilon_k^2 \sin^2 2\phi_k}{\sigma_k^2} U ,$$

where $\sum$ denotes a sum over index k of the n polarizer observations. In other words, again we have a set of three equations in three unknowns. It is very similar in form to the set of three equations for the three-polarizer case solved above and, in fact, is identical if we define a set of "effective three-polarizer characteristics" using these weighted sums.

That is, the three terms on the left hand side of the equals signs can be used as (I_1, I_2, I_3) in equation (1) above. Label these new parameters as I_k'', to get the new three-component vector of effective measurements:

$$I_1'' = \sum \frac{I_k t_k}{\sigma_k^2} , \qquad I_2'' = \sum \frac{I_k t_k \epsilon_k \cos 2\phi_k}{\sigma_k^2} , \qquad I_3'' = \sum \frac{I_k t_k \epsilon_k \sin 2\phi_k}{\sigma_k^2} .$$

Similarly, we can define a three-component vector of effective transmittances:

$$t_1'' = \sum \frac{t_k^2}{\sigma_k^2} , \qquad t_2'' = \sum \frac{t_k^2 \epsilon_k \cos 2\phi_k}{\sigma_k^2} , \qquad t_3'' = \sum \frac{t_k^2 \epsilon_k \sin 2\phi_k}{\sigma_k^2} ,$$

a vector of effective efficiencies:

$$\epsilon_1'' = \frac{1}{\sum t_k^2/\sigma_k^2} \sqrt{\left(\sum \frac{t_k^2}{\sigma_k^2} \epsilon_k \cos 2\phi_k\right)^2 + \left(\sum \frac{t_k^2}{\sigma_k^2} \epsilon_k \sin 2\phi_k\right)^2} ,$$

$$\epsilon_2'' = \frac{1}{\sum t_k^2 \epsilon_k \cos 2\phi_k/\sigma_k^2} \sqrt{\left(\sum \frac{t_k^2}{\sigma_k^2} \epsilon_k^2 \cos^2 2\phi_k\right)^2 + \left(\sum \frac{t_k^2}{\sigma_k^2} \epsilon_k^2 \sin 2\phi_k \cos 2\phi_k\right)^2} ,$$

$$\epsilon_3'' = \frac{1}{\sum t_k^2 \epsilon_k \sin 2\phi_k/\sigma_k^2} \sqrt{\left(\sum \frac{t_k^2}{\sigma_k^2} \epsilon_k^2 \sin 2\phi_k \cos 2\phi_k\right)^2 + \left(\sum \frac{t_k^2}{\sigma_k^2} \epsilon_k^2 \sin^2 2\phi_k\right)^2} ,$$

and a vector of effective "position angles":

$$\begin{aligned}
\phi_1'' &= \frac{1}{2} \tan^{-1} \left(\sum \frac{t_k^2}{\sigma_k^2} \epsilon_k \sin 2\phi_k \Big/ \sum \frac{t_k^2}{\sigma_k^2} \epsilon_k \cos 2\phi_k\right) , \\
\phi_2'' &= \frac{1}{2} \tan^{-1} \left(\sum \frac{t_k^2}{\sigma_k^2} \epsilon_k^2 \sin 2\phi_k \cos 2\phi_k \Big/ \sum \frac{t_k^2}{\sigma_k^2} \epsilon_k^2 \cos^2 2\phi_k\right) , \\
\phi_3'' &= \frac{1}{2} \tan^{-1} \left(\sum \frac{t_k^2}{\sigma_k^2} \epsilon_k^2 \sin^2 2\phi_k \Big/ \sum \frac{t_k^2}{\sigma_k^2} \epsilon_k^2 \sin 2\phi_k \cos 2\phi_k\right) .
\end{aligned}$$

By making these substitutions, the solution given by equations (3) and (4) can be used immediately. Although they appear somewhat messy, in fact, there are rather few sums over terms and the coding is straightforward. That is, a set of observations with n polarizers *can be made equivalent to a set of observations through three polarizers.*

In the actual case of $n = 3$, it can also be shown that the maximum likelihood or least-squares solution is identical to the direct matrix inversion used for the three-polarizer case.

The error analysis (i.e., derivation of the covariance matrix) also follows from this analysis. Returning to the original maximum likelihood formalism, the curvature matrix of χ^2 with respect to (I, Q, U) can be calculated by differentiating equation (7) twice this time to obtain

$$\frac{\partial^2\chi^2}{\partial I^2} = \sum \frac{t_k^2}{4\sigma_k^2}\,, \qquad \frac{\partial^2\chi^2}{\partial Q^2} = \sum \frac{t_k^2}{4\sigma_k^2}\,\epsilon_k^2 \cos^2 2\phi_k\,, \qquad \frac{\partial^2\chi^2}{\partial U^2} = \sum \frac{t_k^2}{4\sigma_k^2}\,\epsilon_k^2 \sin^2 2\phi_k\,;$$

$$\frac{\partial^2\chi^2}{\partial I \partial Q} = \frac{\partial^2\chi^2}{\partial Q \partial I} = \sum \frac{t_k^2}{4\sigma_k^2}\,\epsilon_k \cos 2\phi_k\,, \qquad \frac{\partial^2\chi^2}{\partial I \partial U} = \frac{\partial^2\chi^2}{\partial U \partial I} = \sum \frac{t_k^2}{4\sigma_k^2}\,\epsilon_k \sin 2\phi_k\,,$$

$$\frac{\partial^2\chi^2}{\partial Q \partial U} = \frac{\partial^2\chi^2}{\partial U \partial Q} = \sum \frac{t_k^2}{4\sigma_k^2}\,\epsilon_k^2 \sin 2\phi_k \cos 2\phi_k\,.$$

Casting in matrix form,

$$C = \begin{pmatrix} \dfrac{\partial^2\chi^2}{\partial I^2} & \dfrac{\partial^2\chi^2}{\partial I \partial Q} & \dfrac{\partial^2\chi^2}{\partial I \partial U} \\ \dfrac{\partial^2\chi^2}{\partial Q \partial I} & \dfrac{\partial^2\chi^2}{\partial Q^2} & \dfrac{\partial^2\chi^2}{\partial Q \partial U} \\ \dfrac{\partial^2\chi^2}{\partial U \partial I} & \dfrac{\partial^2\chi^2}{\partial U \partial Q} & \dfrac{\partial^2\chi^2}{\partial U^2} \end{pmatrix}. \tag{8}$$

Then the covariance matrix of the solution to this system is the inverse of C. While in principle that matrix could be calculated analytically, it is probably easier to carry out the matrix inversion numerically having first evaluated the various sums of terms required.

5. DEBIASING PROCEDURE FOR POLARIZED FLUX

At this point, we conclude our analysis of derivation of the Stokes parameters from a set of input observations, a crucial first stage in polarization analysis. We have shown how to obtain the solution for the Stokes parameters in all cases and how to calculate the associated covariance matrix appropriate to that solution. We now wish to use this information to derive the polarization degree and position angle of polarization. We assume that as input we have the Stokes parameters and their covariance matrix. The number of observations and their individual measurements and errors no longer enter the problem.

5.1. Geometric Visualization

If one makes repeated observations of a polarized light source, then, subject to the above assumptions, the derived Stokes parameters will form a cloud of points in (I, Q, U)-space. For the moment, just consider the (Q, U)-plane. The distribution of points will have a mean value which approaches the underlying intrinsic (Q_0, U_0)-values of the source. They will scatter around that mean value as a bivariate normal distribution, with dispersion in the Q-axis of σ_Q and in the U-axis by σ_U. In general, the data points will be correlated, with a correlation coefficient given by

$$R_{QU} = \frac{\sigma_{QU}^2}{\sigma_Q \sigma_U} = \frac{v_{QU}}{\sqrt{v_Q v_U}}\,,$$

where v_{QU} is the covariance between Q and U and v_Q, v_U are the variances of Q and U. The dispersion of the points and their correlation depends on the S/N of the data and the characteristics of the polarizers. Figure 1 illustrates.

Estimation of the polarized flux Ip is equivalent to estimating the length of the radius vector from the origin to the center of the distribution (Q_0, U_0), and estimation of the polarization position angle θ is equivalent to measuring the polar angle 2θ of that vector from the Q-axis. It is well known that simply using the individual measurements (Q_i, U_i) and taking $(Q_i^2 + U_i^2)^{1/2}$ as the estimate of the radius results in a biased estimate, since the positive definite sum of squares always causes random deviations to add statistically to the result. This is most easily seen if the true center of the distribution lies at the origin, i.e., the source is unpolarized. All measurements of radius from the origin give positive values (see, e.g., Serkowski 1958; Wardle & Kronberg 1974; Simmons & Stewart 1985; Clarke & Stewart 1986).

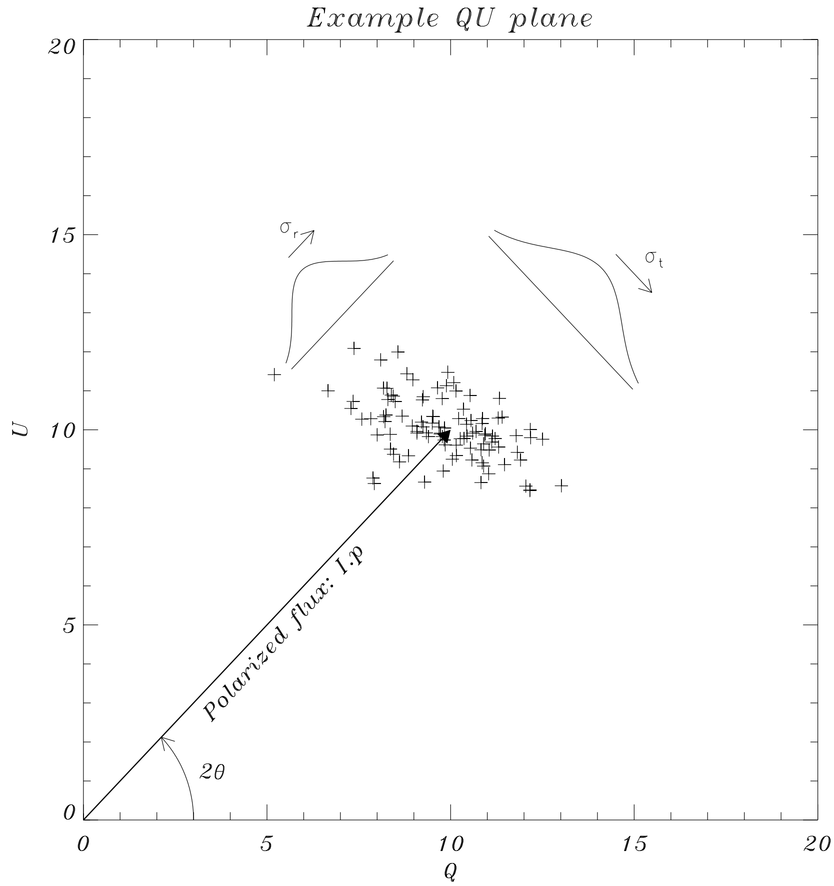

FIG. 1.—Sketch of possible distribution of repeated measurements in the (Q, U)-plane, with correlations that might arise from use of imperfect polarizers

Here, we show that by rotating and rescaling using the covariance matrix, the Stokes parameters can be transformed into uncorrelated, unit-variance normally distributed data, for which the distribution of radii obeys the Rice distribution, $F(p, p_0) = pe^{-[(p^2+p_0^2)/2]}I_0(pp_0)$, where I_0 is the zero-order Bessel function, using the notation of Simmons & Stewart (1985), and p and p_0 are the observed and true degrees of polarization, that is, $p = (Q_i^2 + U_i^2)^{1/2}$ and $p_0 = (Q_0^2 + U_0^2)^{1/2}$. Note that while conceptually the underlying distribution of the data is described in these ways, in practice for panoramic polarization measurement we seldom have more than one or a few measurements within the distribution.

Given data in this standardized form, a choice of estimators and techniques is available to correct for the positive definite bias. Here, for our Monte Carlo simulations, we use the mean of the distribution, as in Serkowski (1958). Simmons & Stewart (1985) advocate the use of the maximum likelihood estimator, while Wardle & Kronberg (1974) propose the use of the distribution peak. All three of these are given as tables in the Appendix.

An interesting property of the bivariate normal distribution is that even in the presence of correlation between the variables, the *projected* dispersions do *not* involve the correlation and are given by the usual σ_Q and σ_U. We will use this in rescaling the variables and, again, later in our error estimation.

5.2. Stokes Parameter Transformations

The bivariate Gaussian $g(x, y)$ is given by

$$g(x, y) = \frac{1}{2\pi\sigma_x\sigma_y\sqrt{1-R^2}} \exp\left\{-\frac{1}{2(1-R^2)}\left[\frac{(x-x_0)^2}{\sigma_x^2} + \frac{(y-y_0)^2}{\sigma_y^2} - 2R\,\frac{(x-x_0)(y-y_0)}{\sigma_x\sigma_y}\right]\right\},$$

where R is the usual correlation coefficient between the two variables. For our example, $Q \equiv x$, $U \equiv y$ and $\sigma_Q \equiv \sigma_x$, $\sigma_U \equiv \sigma_y$, $R = \sigma_{QU}^2/\sigma_Q\sigma_U$.

We can eliminate the correlation in these data by rotating the axes through an angle ζ' given by

$$\zeta' = \frac{1}{2} \tan^{-1} \left(\frac{2R\sigma_Q \sigma_U}{\sigma_Q^2 - \sigma_U^2} \right)$$

to coordinates (x', y'), say. The correlation coefficient becomes zero (rotating to the principal axes of the distribution). For completeness, for an arbitrary rotation through angle ζ,

$$R' = [\sin 2\zeta(\sigma_y^2 - \sigma_x^2) + 2R\sigma_x \sigma_y \cos 2\zeta]/2\sigma'_x \sigma'_y \, ,$$

$$x' = x \cos \zeta + y \sin \zeta \, , \qquad y' = y \cos \zeta - x \sin \zeta \, .$$

In those coordinates, the dispersions in x' and y' are given by

$$\sigma_x'^2 = \sigma_x^2 \cos^2 \zeta + \sigma_y^2 \sin^2 \zeta + R\sigma_x \sigma_y \sin 2\zeta \, , \qquad \sigma_y'^2 = \sigma_x^2 \sin^2 \zeta + \sigma_y^2 \cos^2 \zeta - R\sigma_x \sigma_y \sin 2\zeta \, .$$

Then, rescaling the coordinates according to

$$x'' = x'/\sigma'_x \, , \qquad y'' = y'/\sigma'_y \, ,$$

we have a set of data points whose underlying distribution has unit variance in both axes and no correlation between the variables.

This simplifies the bias estimation problem, since we are now in well-trodden territory. The estimates of radii follow the Rice distribution, above, and given the standardized nature of the new variables, the chosen correction function can be evaluated once and for all and used as a lookup table. Hereafter, we sketch the subsequent analysis and refer the reader to Clarke & Stewart (1986) for much more detail.

As our estimate of the bias, we adopt the mean correction that would be appropriate if our measurement were at the distribution center (Serkowski 1958):

$$r''_c = r'' - b(r'') \, , \qquad \text{where} \qquad b = \frac{1}{2\pi} \int \sqrt{x^2 + y^2} \exp \left\{ -\frac{1}{2} [(x - x_0)^2 + (y - y_0)^2] \right\} dx dy - \sqrt{x_0^2 + y_0^2} \, .$$

The function b is tabulated in the Appendix. Serkowski (1958) gives an analytic expression using confluent hypergeometric functions, with his $\epsilon = 1$. Wardle & Kronberg (1974) use the maximum value of the probability distribution rather than the mean, the mean requiring a rather larger bias correction, while Simmons & Stewart (1985) advocate a maximum likelihood correction. At large S/N all of these corrections approach $b(x) \approx (1 + x^2)^{1/2} - x$.

In these rotated and rescaled coordinates, we take the observed polar angle as our estimate of the actual polar angle, which is unbiased since the distribution is symmetric either side of the mean radius vector.

Hence we have a corrected radius vector r''_c and a polar angle $\xi = \tan^{-1} (y''/x'')$. Running backward now through manipulations equivalent to the transformations above, i.e., scaling and rotating by the factors and angle above, we derive our final estimate of the polarized flux and position angle:

$$x''_c = r''_c \cos \xi \, , \quad y''_c = r''_c \sin \xi \, , \quad x'_c = x''_c \sigma'_x, \quad y'_c = y''_c \sigma'_y \, , \quad x_c = x'_c \cos \zeta - y'_c \sin \zeta \, , \quad y_c = x'_c \sin \zeta + y'_c \cos \zeta \, ,$$

and finally,

$$Ip_c = \sqrt{x_c^2 + y_c^2} \, , \qquad \theta_c = \frac{1}{2} \tan^{-1} (y_c/x_c) \, .$$

Although this may sound complex, in fact, once given the covariance matrix, which we showed how to derive in the first half of the paper, and the function b, which can be tabulated, the operations are quite straightforward manipulations of the data.

6. ERROR ESTIMATION FOR POLARIZED FLUX AND POSITION ANGLE

Returning to Figure 1, we visualize the problem to hand as estimation of the center of the (Q, U) distribution, its radius (the polarized flux), and polar angle (twice the position angle). As noted above, even in the presence of correlation in the data the bivariate normal distribution projects onto a simple one-dimensional normal distribution. We exploit this property to estimate the uncertainty in polarized flux by projecting the distribution onto the radius vector, and the uncertainty on the position angle is obtained in a similar way by projecting the distribution onto the tangent to the radius vector, a procedure analogous to that of Clarke & Stewart (1986).

Explicitly, if the radius vector is at an angle ψ to the Q-axis, and if the dispersions projected onto the Q- and U-axes are, respectively, σ_Q and σ_U, and if the correlation coefficient between Q and U is R (σ and R from the covariance matrix), then the dispersions along the radius vector and tangent are, respectively,

$$\sigma_r^2 = \sigma_Q^2 \cos^2 \psi + \sigma_U^2 \sin^2 \psi + R\sigma_Q \sigma_U \sin 2\psi\ , \qquad \sigma_t^2 = \sigma_Q^2 \sin^2 \psi + \sigma_U^2 \cos^2 \psi - R\sigma_Q \sigma_U \sin 2\psi\ .$$

We can use our estimate σ_r directly as an estimate of the uncertainty on the polarized flux, Ip, and the uncertainty on the derived polar angle will be $\sigma_t/(Ip)$, leading to $\sigma(\theta) = 0.5\sigma_t/(Ip)$. The corresponding uncertainty on the degree of polarization p we take as σ_r/I.

7. MONTE CARLO SIMULATION

7.1. Setup Procedures

In order to check for consistency in approach, to test the efficacy of the debiasing procedure, and to validate the error formulae, a series of Monte Carlo simulations were run for the case of three perfect polarizers.

A single run required specification of the underlying polarization and position angle, along with the appropriate characterization of polarizers (assumed known). First, the underlying or correct value of the triplet (I_1, I_2, I_3) was calculated. These represent the underlying error-free observables. To simulate actual observations, we allow an uncertainty σ_i on each component and draw typically 1000 trials at random from either a normal or Poisson distribution. Each trial represents a simulated observation which can be processed through the formalism above to estimate polarization, position angle, and so on. The dispersion of simulated measurements can, for example, be compared with the mean dispersion resulting from the analytic expressions.

Simulations were calculated for a range of intrinsic polarization degree and S/N in the data. Given that lower S/N data are needed to measure higher polarizations, it seems reasonable to compare derived accuracies to the parameter $\eta \equiv p\langle \mathrm{S/N} \rangle$. This is done below in § 7.4.

7.2. Validation of the Error Analysis

Figure 2 shows the dispersion of calculated Stokes parameters in the simulations compared with the mean of the analytically calculated dispersions. Each plotted point represents 1000 random simulated observations for a single set of input polarization parameters. There are 150 different combinations of polarization parameters corresponding to the 150 plotted points. The analytic formulae work well for the variances and covariances of the Stokes parameters. Essentially identical results are found for Gaussian and Poisson statistics, except that in the Gaussian case all uncertainties are the same and the covariances go to zero, while for Poisson statistics (shown) a nonzero covariance arises from the different uncertainties on each observation.

Figure 3 shows the dispersions of calculated polarization degree and position angle compared with the mean of the analytically calculated uncertainty. Again, the agreement is quite good.

7.3. Effectiveness of the Debiasing Technique

Figures 4 and 5 show the (derived/true) polarization versus η for the raw polarization measurement (no debiasing) and with the debiasing correction, respectively. The debiasing scheme is effective in restoring symmetry to the calculated polarization distribution. For values of $\eta > 10.0$ approximately, the debiasing correction becomes small. For example, if the source is polarized 1%, then this corresponds to an S/N per image of 1000. Another example is that the bias reaches $\sim$20% of the true polarization for $\eta \sim 1.4$. Therefore, for a source polarized 5%, we would suffer significant bias error if the S/N per image is less than $\sim$30.

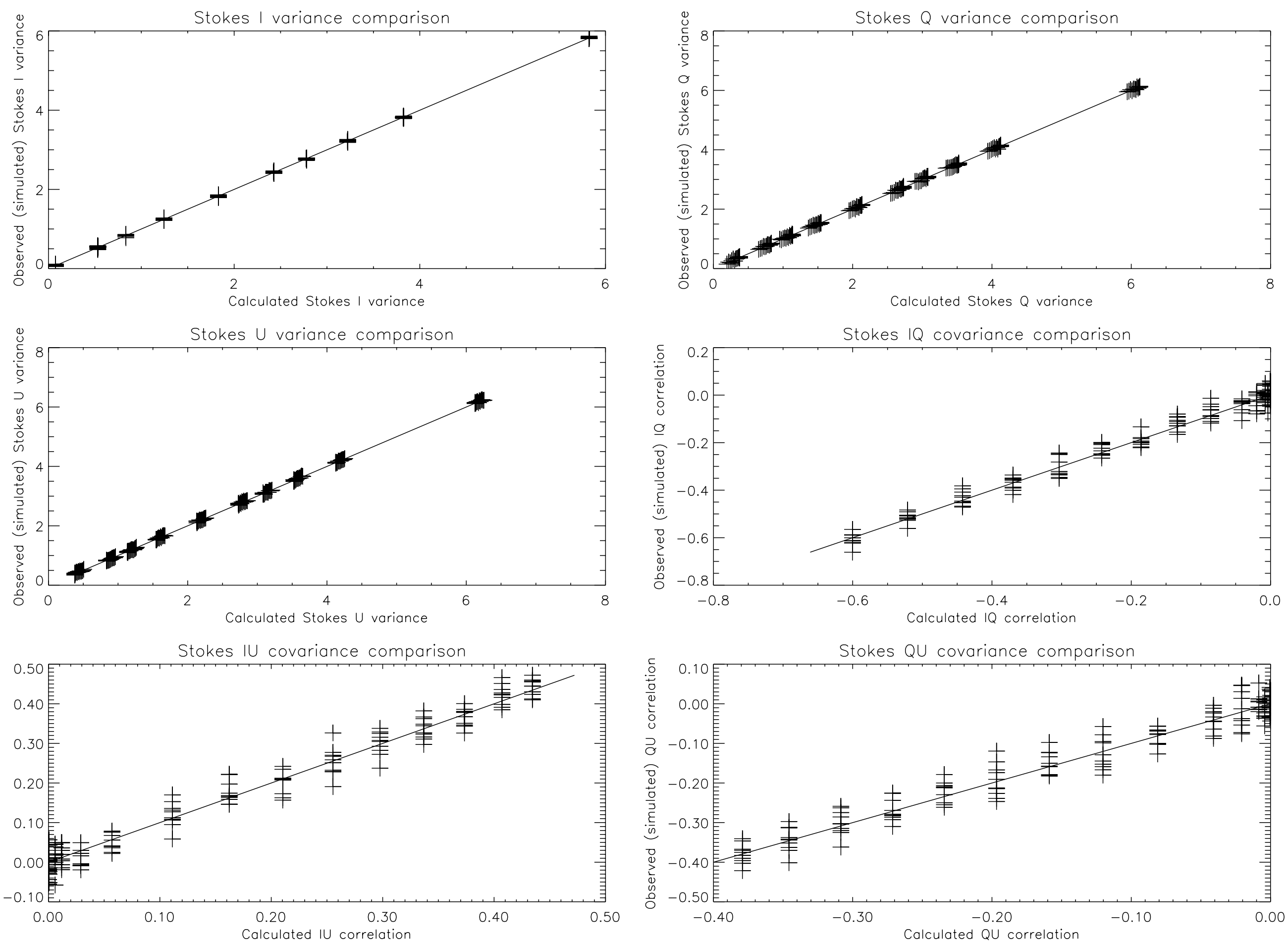

FIG. 2.—Comparison of variances " observed " from the Monte Carlo simulations compared with the mean of the calculated variances. Each plotted point represents 1000 random simulated observations, here using Poisson statistics. The comparison lines have unit slope and zero intercept.

7.4. Application to Observation Design and Achievable Accuracies

Given that lower S/N data are needed to measure higher polarizations to a given accuracy (i.e., we require much higher S/N to measure a polarization level of 0.01% to 30% accuracy than we do to measure a source polarized 50% to 30% accuracy), we compare derived accuracies to $\eta \equiv p\langle S/N \rangle$, where $\langle S/N \rangle$ is the average S/N per image. Figures 6 and 7 show the results of that exercise for the Monte Carlo simulations described above (i.e., three perfect polarizers at optimal orientation).

As expected, the accuracy obtainable is simply a function of this one parameter, for all intents and purposes. In particular the error on the polarization degree is almost just the inverse of the S/N. An excellent fit to the data shown in Figure 6 is

$$\log_{10}(\sigma_p/p) = -0.102 - 0.9898\log_{10}(p\langle S/N \rangle_i) ,$$

where $\langle S/N \rangle_i$ is the average S/N of the three input images. Similarly,

$$\log_{10}\sigma_\theta = 1.415 - 1.068\log_{10}(p\langle S/N \rangle_i)$$

gives an accurate estimate of the uncertainties to be expected in derived position angle. These comparison lines are included on the plots.

For example, if one wishes to measure a source whose polarization is anticipated to be in the vicinity of 10%, $p \approx 0.1$, and if one would like a measurement of the degree of polarization good to 20% (i.e., $\sigma_p \approx 0.02$), then an $\langle S/N \rangle$ per image of $\approx$40 is required.

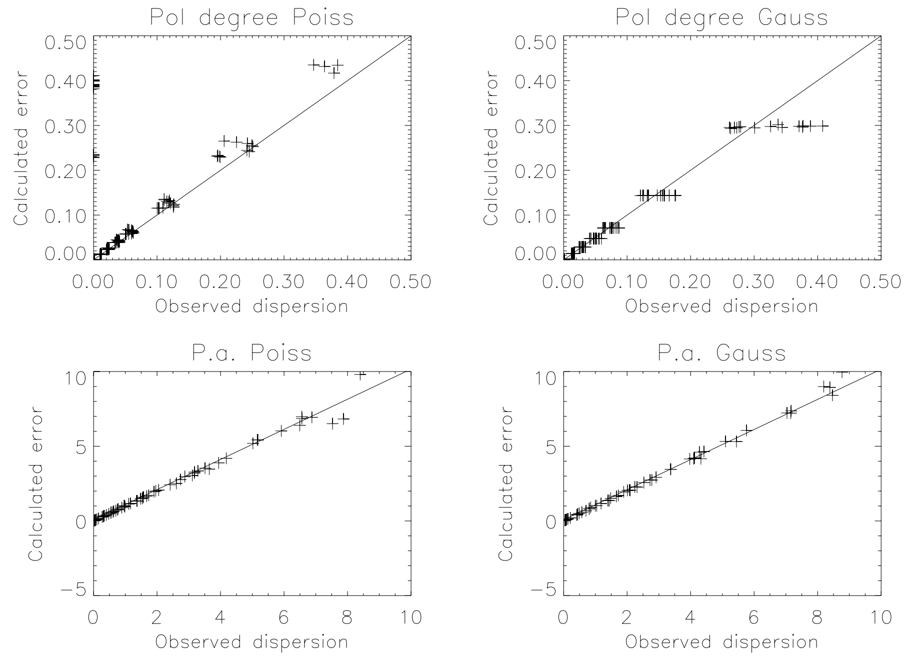

FIG. 3.—Comparison of variances "observed" from the Monte Carlo simulations compared with the mean of the calculated variances for the debiased polarization degree and position angle, for each of Poisson and Gaussian statistics. The comparison lines have unit slope and zero intercept.

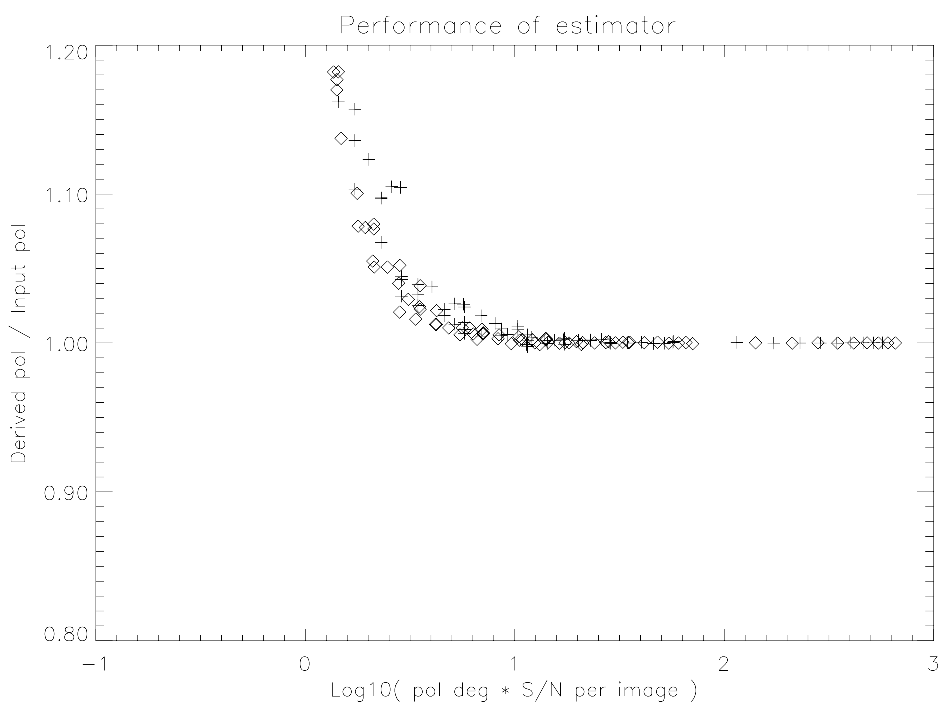

FIG. 4.—Calculated polarization ratio (output divided by input) as a function of polarization times average S/N per image *in the absence of any biasing correction.* For Figs. 4–7, the crosses are for uniform Gaussian uncertainties and the diamonds are for Poisson statistics.

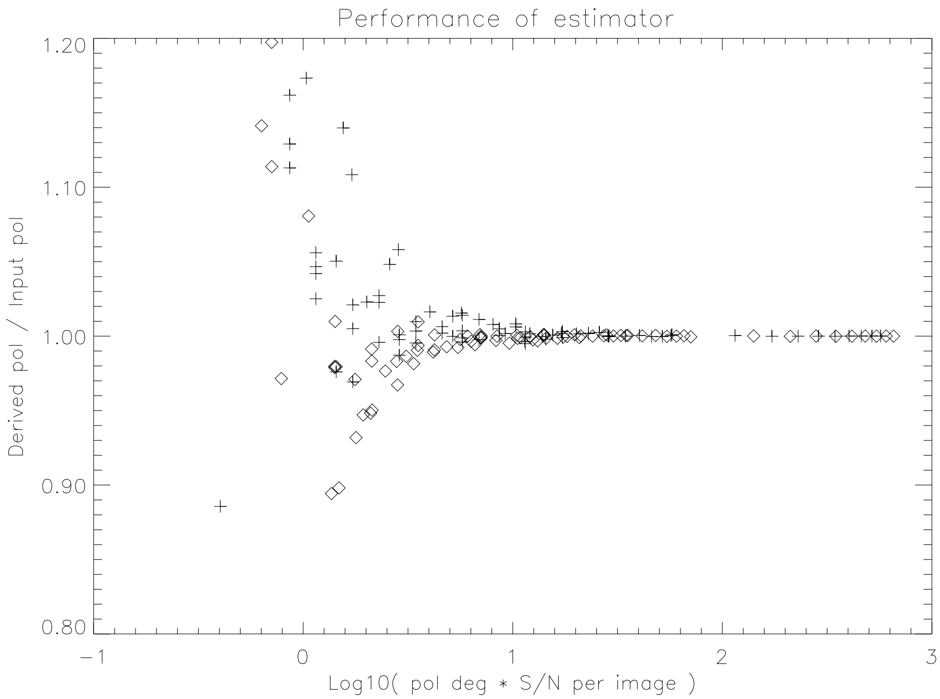

FIG. 5.—Calculated polarization ratio (output divided by input) as a function of polarization times average S/N per image *with biasing correction*

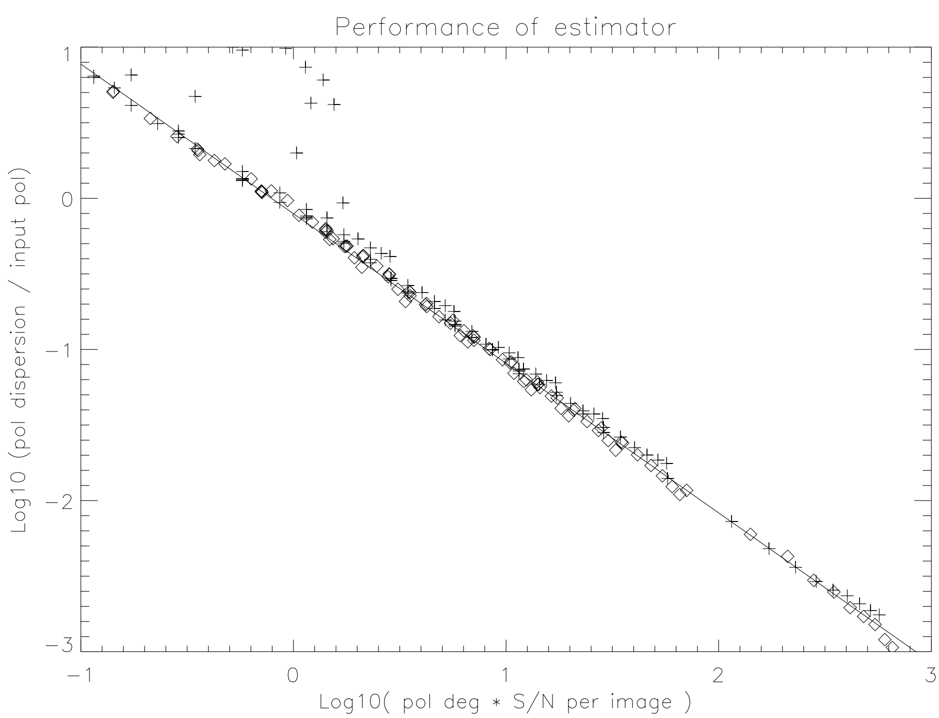

FIG. 6.—Fractional uncertainty in derived polarization as a function of $p\langle S/N\rangle$ for three perfect polarizers. Comparison line is as given in the text.

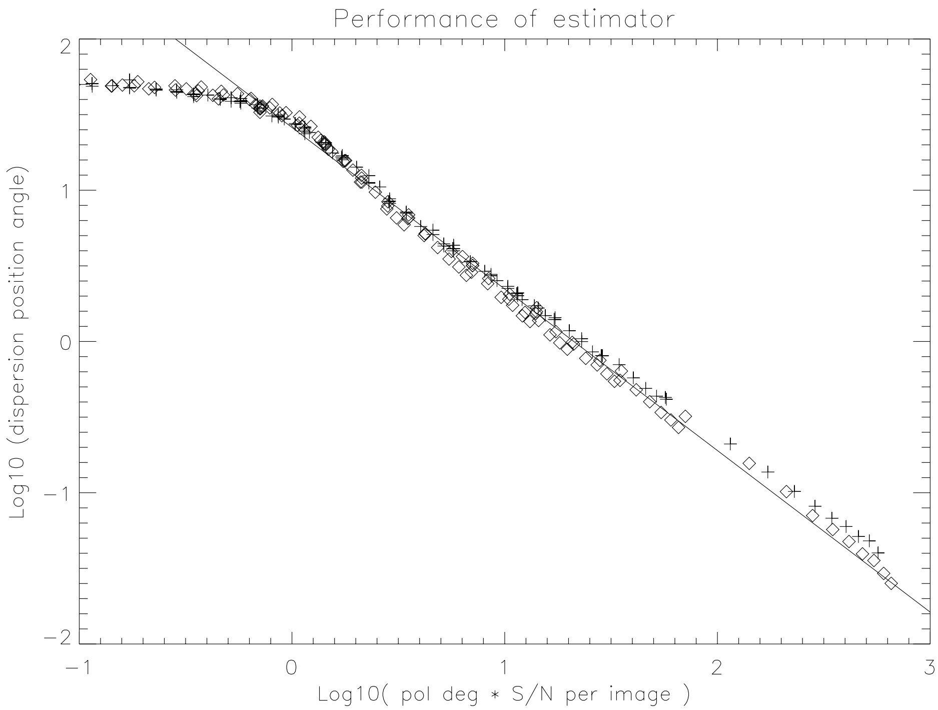

FIG. 7.—Uncertainty in derived position angle (degrees) as a function of $p\langle S/N \rangle$ for three perfect polarizers. The flattening at low $p\langle S/N \rangle$ is due to the position angle becoming essentially undefined, that is, uniformly distributed within 180° expressed as a standard deviation. Comparison line is as given in the text.

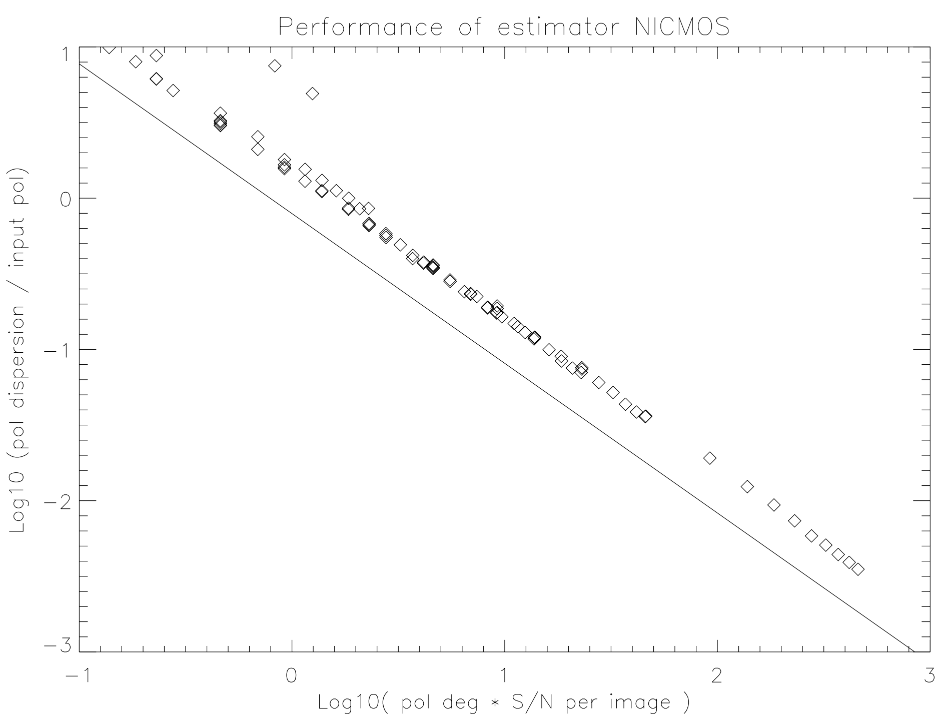

FIG. 8.—Fractional uncertainty in derived polarization as a function of $p\langle S/N \rangle$ for the NICMOS short-wavelength polarizers assuming Gaussian statistics. Comparison line is for perfect polarizers.

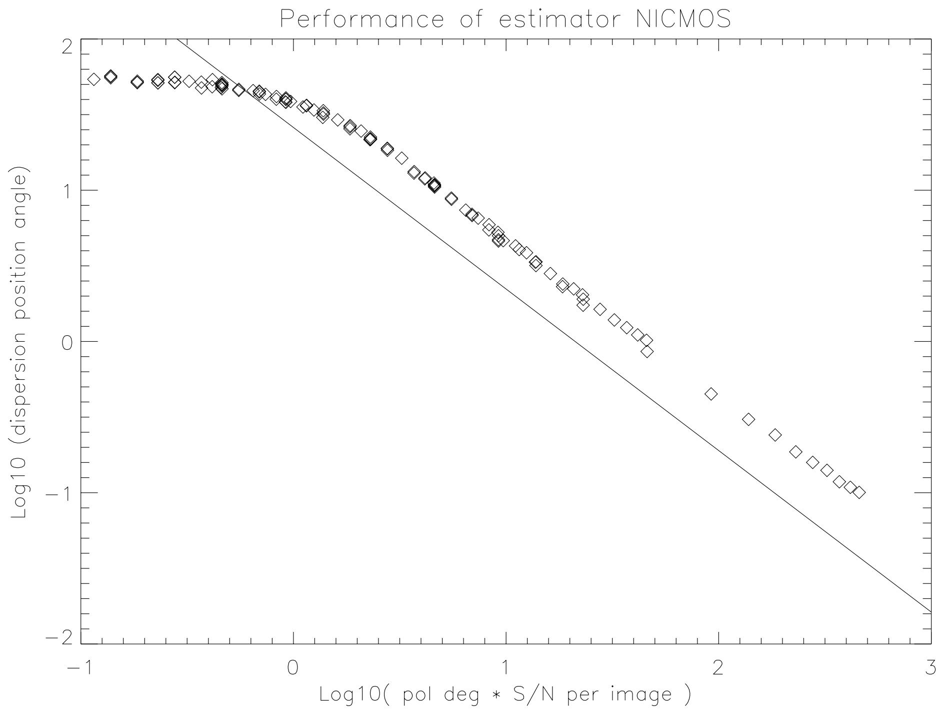

FIG. 9.—Uncertainty in derived position angle (degrees) as a function of $p\langle S/N \rangle$ assuming Gaussian statistics. The flattening at low $p\langle S/N \rangle$ is as in Fig. 7. Comparison line is for perfect polarizers.

As another example, suppose the source is highly polarized, with $p \approx 0.3$ (a 30% polarization), to get an accuracy in position angle of polarization of $\sigma_\theta \approx 10°$, then an $\langle S/N \rangle$ per image of 8 is required.

To obtain a feeling for the amount by which these plots are sensitive to the polarizer characteristics, we also ran a simulation set using uniform Gaussian uncertainties, as above, but this time using the measured characteristics of the NICMOS short-wavelength polarizers (Hines 1998; or see the NICMOS section of the STScI Web site[3]). Figures 8 and 9 show these plots for the NICMOS short-wavelength polarizers using the same comparison lines as for the perfect polarizers. As can be seen, the dispersion in both polarization degree and position angle is offset by close to 0.3 in $\log_{10}$, or a factor of 2 degradation in performance compared with perfect polarizers, as quantified by the uncertainty in observed polarization degree and position angle.

8. CONCLUSIONS

We have presented a rather thorough analysis of the classical problem of observing a source through a general set of polarizing filters and using that information to deduce the corresponding levels of polarization, particularly in the case where the suite of polarizing elements is not perfect.

We have shown that observations with a set of any n polarizers can be expressed as an equivalent set of three-polarizer observations. Formulae have been presented for the variances and covariances of all linear polarization parameters, including the Stokes parameters, degree of polarization, and position angle. Knowledge of the uncertainties in the input data is essential. A way to debias the positive definite polarization degree based on knowledge of the covariances of the Stokes parameters has been offered.

Monte Carlo simulations for the three-polarizer case have been carried out using a variety of input assumptions. Finally, we have shown how these results might be incorporated into experimental design and observational proposals.

The treatment presented here enables accurate recovery of the Stokes parameters from the imperfect WFPC2 and NICMOS polarimeters on *HST*, for example, and is also applicable to the analysis of polarization data from the Advanced Camera for Surveys.

---

[3] See the STScI Web site at http://www.stsci.edu.

We are grateful to Dean Hines for discussions on polarization analysis strategy, particularly with regard to the NICMOS polarization calibration.

APPENDIX

ESTIMATORS AND TECHNIQUES

Tabulation of the bias function for unit-variance uncorrelated observations giving the mean bias that would be measured if the true underlying vector length were r_0. Hence, to debias, the corrected radius $r_c = r_{obs} - b$, where r_{obs} is the observed radius, or in this case transformed polarization, and b is the function tabulated. At small S/N the mean bias function approaches $(\pi/2)^{1/2}$, and at large S/N it approaches $b \approx (1 + x^2)^{1/2} - x$ (see Table A1). Tables A2 and A3 give the equivalent correction functions using the Wardle & Kronberg (1974) distribution peak and Simmons & Stewart (1985) maximum likelihood estimators for completeness. We omit the below-zero thresholding issues discussed by those authors.

TABLE A1

MEAN BIAS FUNCTION FOR TRANSFORMED POLARIZATION OBSERVATIONS

r_0	b	r_0	b	r_0	b	r_0	b
0.000......	1.2533	2.500......	0.2112	5.000......	0.1011	7.500......	0.0670
0.100......	1.1564	2.600......	0.2021	5.100......	0.0990	7.600......	0.0661
0.200......	1.0658	2.700......	0.1938	5.200......	0.0971	7.700......	0.0652
0.300......	0.9813	2.800......	0.1861	5.300......	0.0952	7.800......	0.0644
0.400......	0.9029	2.900......	0.1791	5.400......	0.0934	7.900......	0.0636
0.500......	0.8304	3.000......	0.1726	5.500......	0.0917	8.000......	0.0628
0.600......	0.7636	3.100......	0.1666	5.600......	0.0900	8.100......	0.0620
0.700......	0.7023	3.200......	0.1610	5.700......	0.0884	8.200......	0.0612
0.800......	0.6462	3.300......	0.1557	5.800......	0.0869	8.300......	0.0605
0.900......	0.5951	3.400......	0.1509	5.900......	0.0854	8.400......	0.0597
1.000......	0.5486	3.500......	0.1463	6.000......	0.0839	8.500......	0.0590
1.100......	0.5064	3.600......	0.1420	6.100......	0.0826	8.600......	0.0583
1.200......	0.4683	3.700......	0.1380	6.200......	0.0812	8.700......	0.0577
1.300......	0.4339	3.800......	0.1342	6.300......	0.0799	8.800......	0.0570
1.400......	0.4028	3.900......	0.1306	6.400......	0.0786	8.900......	0.0564
1.500......	0.3749	4.000......	0.1272	6.500......	0.0774	9.000......	0.0557
1.600......	0.3498	4.100......	0.1240	6.600......	0.0762	9.100......	0.0551
1.700......	0.3273	4.200......	0.1209	6.700......	0.0751	9.200......	0.0545
1.800......	0.3070	4.300......	0.1180	6.800......	0.0739	9.300......	0.0539
1.900......	0.2888	4.400......	0.1152	6.900......	0.0729	9.400......	0.0534
2.000......	0.2724	4.500......	0.1126	7.000......	0.0718	9.500......	0.0528
2.100......	0.2576	4.600......	0.1101	7.100......	0.0708	9.600......	0.0522
2.200......	0.2442	4.700......	0.1077	7.200......	0.0698	9.700......	0.0517
2.300......	0.2321	4.800......	0.1054	7.300......	0.0688	9.800......	0.0512
2.400......	0.2212	4.900......	0.1032	7.400......	0.0679	9.900......	0.0506

TABLE A2

WARDLE & KRONBERG (1974) BIAS FUNCTION FOR TRANSFORMED POLARIZATION OBSERVATIONS

r_0	b	r_0	b	r_0	b	r_0	b
0.000......	1.0000	2.500......	0.1783	5.000......	0.0971	7.500......	0.0658
0.100......	0.9025	2.600......	0.1729	5.100......	0.0953	7.600......	0.0650
0.200......	0.8101	2.700......	0.1678	5.200......	0.0936	7.700......	0.0641
0.300......	0.7230	2.800......	0.1629	5.300......	0.0919	7.800......	0.0633
0.400......	0.6416	2.900......	0.1582	5.400......	0.0903	7.900......	0.0625
0.500......	0.5665	3.000......	0.1538	5.500......	0.0887	8.000......	0.0618
0.600......	0.4982	3.100......	0.1496	5.600......	0.0872	8.100......	0.0610
0.700......	0.4377	3.200......	0.1456	5.700......	0.0857	8.200......	0.0603
0.800......	0.3857	3.300......	0.1417	5.800......	0.0843	8.300......	0.0596
0.900......	0.3428	3.400......	0.1381	5.900......	0.0830	8.400......	0.0589
1.000......	0.3091	3.500......	0.1346	6.000......	0.0816	8.500......	0.0582
1.100......	0.2843	3.600......	0.1313	6.100......	0.0804	8.600......	0.0576
1.200......	0.2668	3.700......	0.1281	6.200......	0.0791	8.700......	0.0569
1.300......	0.2548	3.800......	0.1251	6.300......	0.0779	8.800......	0.0563
1.400......	0.2462	3.900......	0.1222	6.400......	0.0767	8.900......	0.0557
1.500......	0.2394	4.000......	0.1194	6.500......	0.0756	9.000......	0.0551
1.600......	0.2333	4.100......	0.1168	6.600......	0.0745	9.100......	0.0545
1.700......	0.2273	4.200......	0.1142	6.700......	0.0734	9.200......	0.0539
1.800......	0.2212	4.300......	0.1118	6.800......	0.0724		
1.900......	0.2149	4.400......	0.1094	6.900......	0.0713		
2.000......	0.2085	4.500......	0.1071	7.000......	0.0704		
2.100......	0.2021	4.600......	0.1050	7.100......	0.0694		
2.200...........	0.1959	4.700......	0.1029	7.200......	0.0685		
2.300......	0.1898	4.800......	0.1009	7.300......	0.0675		
2.400......	0.1839	4.900......	0.0990	7.400......	0.0667		

TABLE A3

MAXIMUM LIKELIHOOD BIAS FUNCTION FOR TRANSFORMED POLARIZATION OBSERVATIONS

r_0	b	r_0	b	r_0	b	r_0	b
0.000......	1.4142	2.500......	0.2089	5.000......	0.1010	7.500......	0.0670
0.100......	1.3160	2.600......	0.2001	5.100......	0.0990	7.600......	0.0661
0.200......	1.2213	2.700......	0.1921	5.200......	0.0971	7.700......	0.0652
0.300......	1.1303	2.800......	0.1847	5.300......	0.0952	7.800......	0.0644
0.400......	1.0430	2.900......	0.1779	5.400......	0.0934	7.900......	0.0635
0.500......	0.9595	3.000......	0.1716	5.500......	0.0917	8.000......	0.0627
0.600......	0.8802	3.100......	0.1657	5.600......	0.0900	8.100......	0.0620
0.700......	0.8052	3.200......	0.1603	5.700......	0.0884	8.200......	0.0612
0.800......	0.7347	3.300......	0.1552	5.800......	0.0869	8.300......	0.0605
0.900......	0.6690	3.400......	0.1504	5.900......	0.0854	8.400......	0.0597
1.000......	0.6083	3.500......	0.1459	6.000......	0.0839	8.500......	0.0590
1.100......	0.5528	3.600......	0.1417	6.100......	0.0825	8.600......	0.0583
1.200......	0.5027	3.700......	0.1377	6.200......	0.0812	8.700......	0.0577
1.300......	0.4580	3.800......	0.1339	6.300......	0.0799	8.800......	0.0570
1.400......	0.4184	3.900......	0.1304	6.400......	0.0786	8.900......	0.0563
1.500......	0.3839	4.000......	0.1270	6.500......	0.0774	9.000......	0.0557
1.600......	0.3539	4.100......	0.1238	6.600......	0.0762	9.100......	0.0551
1.700......	0.3279	4.200......	0.1208	6.700......	0.0750	9.200......	0.0545
1.800......	0.3055	4.300......	0.1179	6.800......	0.0739	9.300......	0.0539
1.900......	0.2860	4.400......	0.1151	6.900......	0.0728	9.400......	0.0533
2.000......	0.2690	4.500......	0.1125	7.000......	0.0718		
2.100......	0.2541	4.600......	0.1100	7.100......	0.0708		
2.200......	0.2409	4.700......	0.1076	7.200......	0.0698		
2.300......	0.2291	4.800......	0.1053	7.300......	0.0688		
2.400......	0.2185	4.900......	0.1031	7.400......	0.0679		

REFERENCES

Antonucci, R. R. J., & Miller, J. S. 1985, ApJ, 297, 621
Axon, D. J., & Ellis, R. S. 1976, MNRAS, 177, 499
Bailey, J., Chrysostomou, A., Hough, J. H., Gledhill, T. M., McCall, A., Clark, S., Menard, F., & Tamura, M. 1998, Science, 281, 672
Biretta, J., & McMaster, M. 1997, WFPC-2 Instrument Science Report 97-11 (Baltimore: STScI)
Capetti, A., Macchetto, F., Axon, D. J., Sparks, W. B., & Boksenberg, A. 1995, ApJ, 452, L87
Clarke, D., & Stewart, B. G. 1986, Vistas Astron., 29, 27
Collett, E. 1993, Polarized Light: Fundamentals and Applications (New York: Marcel Decker)
Ford, H. C., et al. 1998, Proc. SPIE, 3356, 234
Gledhill, T. M., Chrysostomou, A., & Hough, J. H. 1996, MNRAS, 282, 1418
Henney, W. J., Raga, A. C., & Axon, D. J. 1994, ApJ, 427, 305
Hines, D. C. 1998, in ESO Conf. Workshop Proc. 55, NICMOS and the VLT, ed. W. Freudling & R. Hook (Garching: ESO), 63
Hough, J. H., Peacock, T., & Bailey, J. A. 1991, MNRAS, 248, 74
Mathewson, D. S., & Ford, V. L. 1971, MNRAS, 153, 525
Mazzuca, L., Sparks, W. B., & Axon, D. 1998, Instrument Science Report NICMOS 98-017 (Baltimore: STScI)
Nota, A., Jedrzejewski, R., Voit, M., & Hack, W. 1996, FOC Instrument Handbook, Version 7.0 (Baltimore: STScI)
Perlman, E., Biretta, J., Zhou, F., Sparks, W. B., & Macchetto, D. 1999, AJ, 117, 2185
Scarrott, S. M., Warren-Smith, R. F., Pallister, W. S., Axon, D. J., & Bingham, R. G. 1983, MNRAS, 204, 1163
Schmidt, B. P., Kirshner, R. P., Leibundgut, B., Wells, L. A., Porter, A., Ruiz-Lapuente, P., Challis, P., & Filippenko, A. 1994, ApJ, 434, L19
Serkowski, K. 1958, Acta Astron., 8, 135
Simmons, J. F. L., & Stewart, B. G. 1985, A&A, 142, 100
Sparks, W. B. 1994, ApJ, 433, 29
Sparks, W. B., Macchetto, F., Panagia, N., Boffi, F., Branch, D., Hazen, M. L., & Della Valle, M. 1999, ApJ, in press
Sparks, W. B., Miley, G. K., & Macchetto, F. 1990, ApJ, 361, L41
Sparks, W. B., Paresce, F., & Macchetto, F. D. 1989, ApJ, 347, L65
Tinbergen, J. 1996, Astronomical Polarimetry (Cambridge: Cambridge Univ. Press)
Wardle, J. F. C., & Kronberg, P. P. 1974, ApJ, 194, 249